© 2015. Published by The Company of Biologists Ltd | Development (2015) 142, 82-91 doi:10.1242/dev.111039

RESEARCH ARTICLE

A Pak-regulated cell intercalation event leading to a novel radial cell polarity is involved in positioning of the follicle stem cell niche in the *Drosophila* ovary

Stephanie Vlachos[1,*], Sharayu Jangam[1], Ryan Conder[1,‡], Michael Chou[1], Todd Nystul[1,2] and Nicholas Harden[1,§]

ABSTRACT

In the germarium of the *Drosophila* ovary, germline cysts are encapsulated one at a time by a follicular epithelium derived from two follicle stem cells (FSCs). Ovaries in flies mutant for the serine/threonine kinase Pak exhibit a novel phenotype, in which two side-by-side cysts are encapsulated at a time, generating paired egg chambers. This striking phenotype originates in the pupal ovary, where the developing germarium is shaped by the basal stalk, a stack of cells formed by cell intercalation. The process of basal stalk formation is not well understood, and we provide evidence that the cell intercalation is driven by actomyosin contractility of DE-Cadherin-adhered cells, leading to a column of disk-shaped cells exhibiting a novel radial cell polarity. Cell intercalation fails in *Pak* mutant ovaries, leading to abnormally wide basal stalks and consequently wide germaria with side-by-side cysts. We present evidence that *Pak* mutant germaria have extra FSCs, and we propose that contact of a germline cyst with the basal stalk in the pupal ovary contributes to FSC niche formation. The wide basal stalk in *Pak* mutants enables the formation of extra FSC niches which are mispositioned and yet functional, indicating that the FSC niche can be established in diverse locations.

KEY WORDS: *Drosophila*, Ovary, Follicle stem cell, Pak, Cell intercalation, Basal stalk

INTRODUCTION

The germarium, at the anterior end of each ovariole in the *Drosophila* ovary, is a popular structure for the study of stem cell niche formation (Spradling et al., 2008). In the germarium, two or three germline stem cells (GSCs) located at the anterior tip in region 1 (Fig. 1A) give rise to daughter cells, which divide to form cystoblasts. Cystoblasts are encased by escort cells, which move them posteriorly along the germarium by passing them from one escort cell to the next (Morris and Spradling, 2011). Four incomplete divisions in each cystoblast generate a 16-cell germline cyst, which flattens to span the whole width of the germarium in region 2a/2b, halfway down the germarium. Here, cysts encounter two follicle stem cells (FSCs), on opposite sides of the germarium, which encapsulate one cyst at a time in a monolayer of follicle cells (Losick et al., 2011; Nystul and Spradling, 2007) (Fig. 1A,C). The FSC niche is an example of a dynamic epithelial stem cell niche with similarities to niches in other epithelial tissues (Sahai-Hernandez et al., 2012; Sahai-Hernandez and Nystul, 2013). The FSC contributes to formation of its own niche through secretion of the extracellular matrix (ECM) protein Laminin A (LanA), which anchors the FSC to the 2a/2b border and controls FSC proliferation through its function as an integrin ligand (O'Reilly et al., 2008). DE-Cadherin functions to maintain the FSC in the niche by adhering it to the immediately adjacent escort cell (Song and Xie, 2002). The details of how the FSC niche becomes positioned at the 2a/2b border are still being elucidated, although recent studies indicate that it involves intersecting gradients of ligands for the Hedgehog (Hh), Wingless (Wg) and JAK-STAT pathways (Sahai-Hernandez and Nystul, 2013; Vied et al., 2012).

The FSC must be specified before formation of the adult ovary to ensure that the first germline cyst to travel through the germarium is encapsulated into a follicular epithelium. During ovarian development, a mesenchymal cell mass becomes organized into individual ovarioles through the formation of cell stacks by intercalation to form the terminal filaments, basal stalks and interfollicular stalks (Godt and Laski, 1995; Sahut-Barnola et al., 1995). It is likely that the FSC niches become established during these events.

The group I p21-activated kinases (Paks) are important regulators of the F-actin cytoskeleton, and we have been studying the function of Pak in development of the follicular epithelium in the *Drosophila* ovary, where Pak can affect cell shape through the regulation of actomyosin contractility (Conder et al., 2007; Vlachos and Harden, 2011). Here, we characterize a unique phenotype in *Pak* mutant ovarioles bearing age-matched, side-by-side fused egg chambers. These fused egg chambers each have their own complete follicular epithelium, indicating that the *Pak* mutant germarium is capable of encapsulating two cysts at a time instead of the usual one. This suggests that there is extra FSC activity in the *Pak* mutant germarium, and we present evidence that this extra activity is due to supernumerary FSCs occupying supernumerary niches. In searching for the cause of these supernumerary niches, we have determined that *Pak* mutant pupal ovaries have a cell intercalation defect in the formation of the basal stalk, causing it to be wider than normal. In characterizing the basal stalk we have discovered a novel radial cell polarity in the basal stalk cells. We propose that the basal stalk is used to position the first germline cyst during formation of the germarium, and that this cyst positioning contributes to formation of the FSC niche. The wider basal stalk in *Pak* mutant ovaries allows side-by-side positioning of cysts, which might enable formation of supernumerary FSC niches and FSCs. Despite being mislocalized, these supernumerary FSCs are capable of generating a functional follicular epithelium.

[1]Department of Molecular Biology and Biochemistry, Simon Fraser University, Burnaby, British Columbia, Canada V5A 1S6. [2]Departments of Anatomy and OB/GYN-RS, University of California, San Francisco, CA 94143, USA.
*Present address: Departments of Anatomy and OB/GYN-RS, University of California, San Francisco, CA 94143, USA. ‡Present address: STEMCELL Technologies, Vancouver, BC, Canada V5Z 1B3.

§Author for correspondence (nharden@sfu.ca)

Received 8 April 2014; Accepted 9 November 2014

Development (2015) 142, 82-91 doi:10.1242/dev.111039

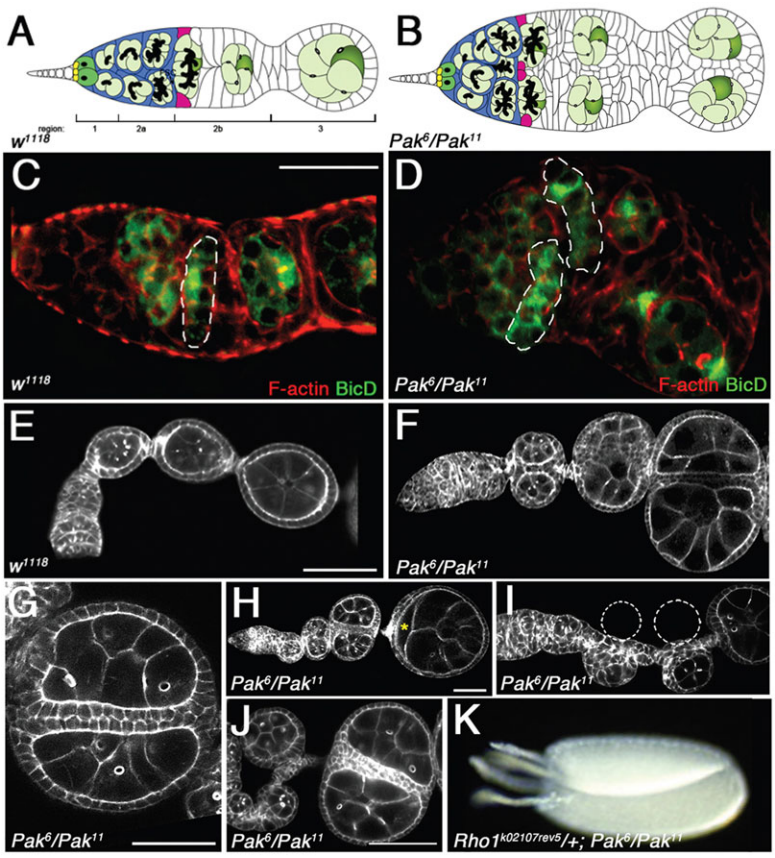

Fig. 1. *Pak* mutants exhibit a novel side-by-side egg chamber phenotype. Anterior is to the left in all panels. (A) Schematic of a wild-type germarium. In regions 1 and 2a, germline cysts (light green) descended from GSCs (dark green) move through escort cells (blue) to the region 2a/2b border, where they encounter a pair of FSCs (magenta). The FSCs package one cyst at a time into a follicular epithelium (white cells) in region 2b to form egg chambers that bud off in region 3. (B) Schematic of *Pak* mutant germarium. Region 1/2a is shorter and wider than in WT. Four FSCs package two cysts at a time to form side-by-side paired egg chambers. Samples in panels C-J were stained with FITC-Phalloidin to outline cells. Samples in panels C,D were additionally stained with anti-BicD to reveal germline cysts. (C) Wild-type germarium showing single, flattened cyst at region 2a/2b boundary (dashed line). (D) Pak^{6}/Pak^{11} germarium showing two flattened cysts at region 2a/2b boundary (dashed lines). (E) Portion of a wild-type ovariole showing a single row of three egg chambers. (F) Portion of Pak^{6}/Pak^{11} ovariole showing three pairs of side-by-side egg chambers. (G) Close-up view of paired, fused egg chambers in Pak^{6}/Pak^{11} ovariole, showing that each egg chamber is encapsulated in its own monolayer of follicle cells. (H) Pak^{6}/Pak^{11} ovariole showing unpaired egg chamber, followed by two pairs of younger, paired egg chambers. Asterisk marks mispositioned oocyte in the unpaired egg chamber. The oocyte is frequently mispositioned in *Pak* mutant ovarioles bearing paired egg chambers. (I) Pak^{6}/Pak^{11} ovariole showing unpaired egg chamber, followed by two younger, unpaired egg chambers on one side of an aberrant stalk. Dashed circles indicate positions of 'missing' partner egg chambers. (J) Portion of Pak^{6}/Pak^{11} ovariole showing paired egg chambers, followed by three younger, unpaired egg chambers positioned on alternating sides of an aberrant stalk. (K) Side-by-side fused eggs, each with a pair of dorsal appendages, from $rho^{k02107rev5}$/+; Pak^{6}/Pak^{11} female. Scale bars: 25 µm in C,D; 50 µm in E-J.

RESULTS

Side-by-side encapsulation of cysts in *Pak* mutant germaria indicates an increase in FSC activity

Females trans-heterozygous for alleles of *Pak* are sterile, with defects in actin cytoskeletal organization and apicobasal polarity in the follicle cells covering egg chambers (Conder et al., 2007). Many *Pak* mutant ovarioles exhibited an additional phenotype of side-by-side, paired egg chambers that was initially evident in the germarium (Fig. 1B,D) and was present throughout the ovariole (Fig. 1F). These paired egg chambers each had a wild-type number of germ cells and their own complete follicular epithelium, such that, at the region of fusion, there was a bilayered epithelium (Fig. 1G). To our knowledge, this striking paired ovariole phenotype has not been reported previously. Side-by-side cysts in the germarium have been described previously, but these are not individually encapsulated as they become egg chambers (Frydman and Spradling, 2001; Gonzalez-Reyes and St Johnston, 1998; Hartman et al., 2010; McCaffrey et al., 2006; Muzzopappa and Wappner, 2005; O'Reilly et al., 2006; Song and Xie, 2003). In most cases, these side-by-side cysts appear to be due to a failure of cysts to flatten at the 2a/2b boundary (Frydman and Spradling, 2001; Gonzalez-Reyes and St Johnston, 1998; McCaffrey et al., 2006; Muzzopappa and Wappner, 2005; O'Reilly et al., 2006). However, this was not the case in *Pak* mutant ovarioles, where side-by-side flattening of cysts occurred (Fig. 1D).

We observed *Pak* mutant ovarioles in which an unpaired egg chamber was followed by paired egg chambers, as well as the occurrence of unpaired egg chambers positioned to one side or the other of an aberrant 'stalk' of follicle cells (Fig. 1H-J). These unpaired egg chambers on the sides of the stalk gave the appearance of being 'paired' egg chambers lacking their partners (Fig. 1I). We quantified the various phenotypes in one-day-old and four-day-old *Pak* mutant adult ovaries to test whether there were any changes in distribution as the fly aged (supplementary material Table S1). Due to the short lifespan of *Pak* mutant adults it was not possible to look at older ovaries. The phenotype of unpaired egg chambers on the side of a stalk was significantly more prevalent in older ovarioles, suggesting that this phenotype emerges as the fly ages (supplementary material Table S1).

Follicle cell types are specified in paired *Pak* mutant egg chambers

Does the FSC produce a fully functional follicular epithelium in the paired egg chambers of *Pak* mutant females? Normally, this cannot be addressed owing to the degradation of all *Pak* chambers at around stage 10 (Conder et al., 2007); however, as we previously demonstrated, heterozygosity for any component of the Rho-activated actomyosin contractility pathway suppresses this degradation (Vlachos and Harden, 2011). Heterozygosity for an allele of *Rho1* enabled a small number of *Pak* mutant paired-egg chambers to develop into fused mature eggs, complete with dorsal appendages (Fig. 1K). Thus, if later *Pak* mutant phenotypes are suppressed, the FSCs in *Pak* mutant ovaries are capable of supplying a normal follicular epithelium to paired egg chambers.

During development of the follicular epithelium, three follicle cell types are specified: main-body follicle cells, polar cells and stalk cells [reviewed by Horne-Badovinac and Bilder (2005)]. The polar cells are pairs of cells at the poles of the egg chamber that are required for specification of the stalk cells, a bridge of disk-shaped cells linking adjacent egg chambers. Failure to specify stalk cells leads to end-to-end fusions of egg chambers, in contrast to the side-by-side fusions seen in *Pak* mutant ovarioles [see e.g. Assa-Kunik

Development (2015) 142, 82-91 doi:10.1242/dev.111039

et al. (2007); Berns et al. (2014); Chen et al. (2011); Hongay and Orr-Weaver (2011); Li et al. (2008); Lopez-Schier and St Johnston (2001); Shyu et al. (2009)]. We examined specification of the polar cells and stalk cells in *Pak* mutant ovarioles by staining for markers that are elevated in these cell types. Anti-FasIII staining revealed the presence of polar cells, but these tended to be aberrantly positioned and variable in number (Fig. 2B). Anti-βPS integrin staining revealed that the stalks linking sets of paired egg chambers in *Pak* mutant ovarioles were wider than in the wild type (WT) and containing more cells, which were frequently organized into two rows of cells in contrast to the normal one row (Fig. 2D). We conclude that the *Pak* mutant side-by-side fused egg chamber phenotype is not caused by loss of stalk cells.

Evidence for extra FSCs in *Pak* mutant germaria

Other mutants producing side-by-side cysts in the germarium do not show paired encapsulation of cysts (Frydman and Spradling, 2001; Gonzalez-Reyes and St Johnston, 1998; Hartman et al., 2010; McCaffrey et al., 2006; Muzzopappa and Wappner, 2005; O'Reilly et al., 2006; Song and Xie, 2003), presumably because they have a wild-type number of FSCs that are incapable of encapsulating two cysts at a time. We searched for evidence of extra FSCs in *Pak* mutant germaria. Excessive JAK-STAT signaling in the germarium leads to the production of putative supernumerary FSCs in inappropriate locations, including βPS integrin-expressing cells located internally in the germarium, distant from the germarial wall (Vied et al., 2012). Internally placed FSCs would be ideally positioned to provide follicle cells at the interface of the paired cysts in *Pak* mutant germaria, and we looked for their presence. Recent studies have identified two markers expressed in FSCs and their progeny: follicle cell nuclear antigens and Castor (Cas). Staining ovaries for either of these markers together with anti-FasIII reveals probable FSCs as positive for the marker but negative for FasIII (Chang et al., 2013; Hartman et al., 2013). We stained wild-type and *Pak* mutant ovarioles with antibodies against Cas and FasIII. Putative FSCs in wild-type germaria were visible as Cas-positive, FasIII-negative cells at the 2a/2b boundary (Fig. 3A-A″). In *Pak* mutant germaria, additional Cas-positive, FasIII-negative cells were consistently seen at the interface of side-by-side cysts (Fig. 3B-C″). FSCs secrete the integrin ligand LanA, which is normally deposited along the germarial cell wall (O'Reilly et al., 2008) (Fig. 3D), whereas in *Pak* mutant germaria, we saw additional, internal LanA accumulation, further evidence for internally positioned FSCs (Fig. 3E). To test the hypothesis that elevated FSC activity enables *Pak* mutant ovarioles to package two cysts at a time, we looked at the effect of reducing FSC activity in *Pak* mutants. Both Hedgehog and JAK-STAT signaling are required for FSC activity in the germarium, and elevated signaling by either pathway results in the accumulation of supernumerary FSC-like cells (Forbes et al., 1996a,b; Hartman et al., 2010; Vied et al., 2012; Zhang and Kalderon, 2000, 2001). We created *Pak* mutant females heterozygous for alleles of *hh* or *hopscotch* (*hop*, which encodes *Drosophila* JAK), and in both cases we observed side-by-side cysts that were encapsulated together into a single follicular epithelium or only partially separated by a bilayer of follicle cells (Fig. 3F-I). To confirm that we were indeed seeing encapsulation of two side-by-side 16-cell cysts and not one 32-cell cyst, we counted the number of ring canals in the oocytes. Oocytes from 32-cell cysts with two oocytes have five ring canals instead of the usual four, with one ring canal connecting the two oocytes (Mata et al., 2000). In *Pak* mutant ovarioles heterozygous for *hop* alleles, the side-by-side oocytes each had four ring canals, indicating that they were derived from separate 16-cell cysts (Fig. 3I,J). These results indicate that the ability of *Pak* mutant germaria to encapsulate side-by-side cysts into separate follicular epithelia is due to excessive FSC activity; if this FSC activity is reduced, some side-by-side cysts are no longer encapsulated individually.

Analysis of *Pak* mutant clones produced results consistent with there being extra FSCs in *Pak* mutant germaria. The ovariole shown in Fig. 3L-L″ is similar to the ovariole shown in Fig. 1I, in that there is a single egg chamber followed by two egg chambers on the side of an aberrant stalk. In wild-type ovarioles, cysts are encapsulated by follicle cells produced by two FSCs in separate niches on opposite sides of the germarium, with equal contributions from each FSC (Nystul and Spradling, 2007, 2010). If a given cyst in *Pak* mutant ovarioles is similarly served by two FSCs, then the FSCs encapsulating the first egg chamber in Fig. 3L-L″ both appear to be GFP positive. However, the aberrant stalk that follows this first cyst is largely GFP negative, as are many of the follicle cells surrounding the two younger egg chambers, suggesting the existence of a third GFP-negative FSC.

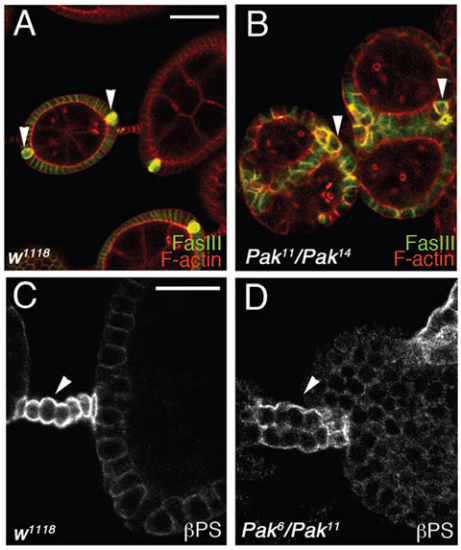

Fig. 2. Polar cells and stalk cells are specified in *Pak* mutant paired egg chambers. (A,B) Phalloidin-stained wild-type (A) and *Pak* mutant ovarioles (B) additionally stained with anti-FasIII to reveal polar cells. Wild-type egg chambers have a pair of polar cells at each pole (arrowheads). Polar cells are specified in *Pak* mutant ovarioles (arrowheads) but vary in position and number. (C,D) Wild-type (C) and *Pak* mutant ovarioles (D) stained with anti-βPS integrin to reveal stalk cells. Stalks in wild-type ovarioles are composed of a single row of cells (arrowhead), whereas paired egg chambers in *Pak* mutants are linked by stalks two rows wide (arrowhead). Scale bars: 50 µm in A for A,B; 25 µm in C for C,D.

The paired egg chamber phenotype is caused by loss of Pak in pre-adult somatic cells

We used clonal analysis and tissue-specific expression of a *Pak* RNAi transgene to determine when and where Pak is required to prevent the side-by-side egg chamber phenotype. This phenotype was never seen when only germline cells were mutant for *Pak*, but could be replicated by loss of Pak in somatic cells when clones were induced in third-instar larvae but not in adults (Fig. 4A; and data not shown). We observed paired egg chambers in which at least one FSC was WT for Pak, indicating that loss of Pak in all FSCs is not

Development (2015) 142, 82-91 doi:10.1242/dev.111039

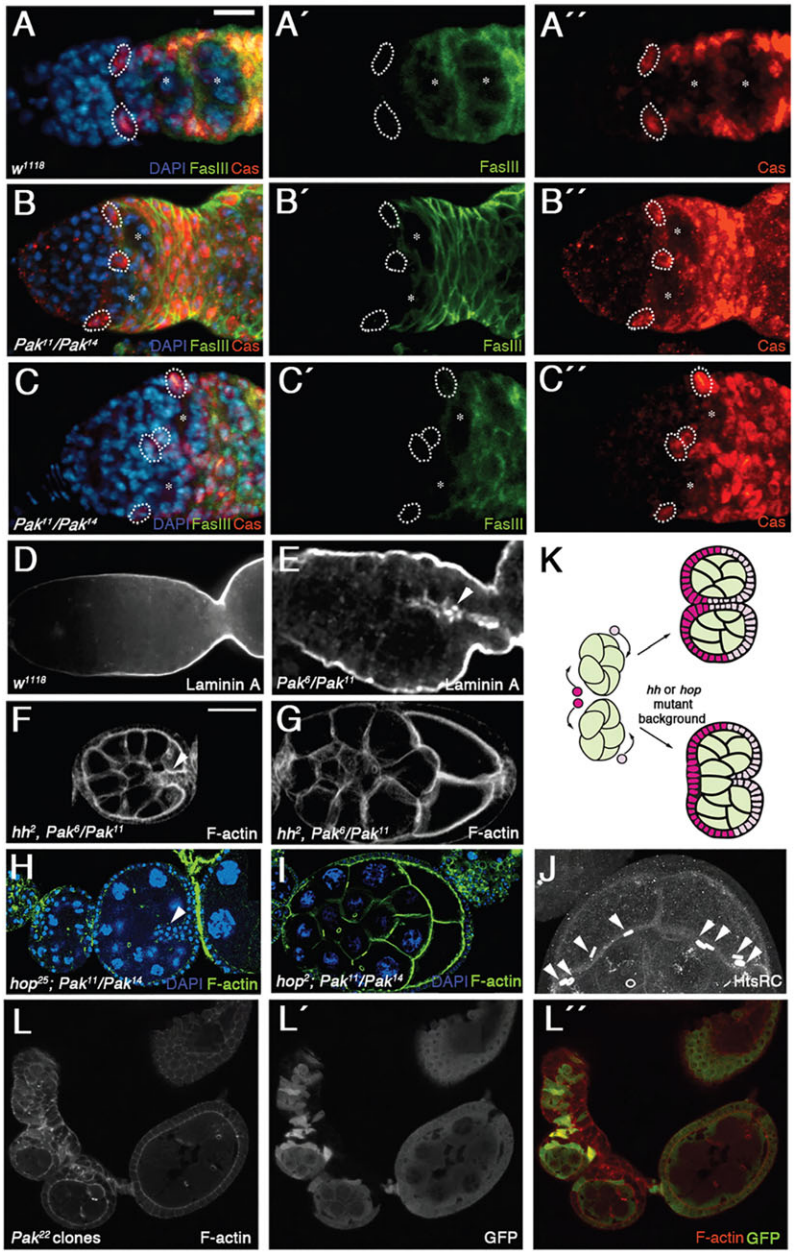

Fig. 3. Evidence for increased FSC activity in *Pak* mutant ovaries. (A-C″) Wild-type (A-A″) and *Pak* mutant (B-C″) germaria stained with DAPI (blue), anti-FasIII (green) and anti-Cas (red). Asterisks mark germline cysts. FasIII-negative, Cas-positive cells are circled by dotted lines. These are probably FSCs, and extra cells of this type are found in *Pak* mutant ovarioles at the interface of side-by-side cysts. (D,E) Wild-type (D) and *Pak* mutant (E) germaria stained with anti-LanA. There is ectopic LanA accumulation in the *Pak* mutant germarium (arrowhead). (F-I) *Pak* mutant egg chambers stained with phalloidin (F,G) or phalloidin and DAPI (H,I), showing that reduction of FSC activity through impairment of Hh or JAK-STAT signaling suppresses separate encapsulation of side-by-side cysts. Side-by-side cysts exhibit either a partial, bilayered epithelium between them (F,H, arrowheads; about 15% of *hop* heterozygous *Pak* mutant ovarioles show this phenotype) or are packaged into a single follicular epithelium (G,I; about 5% of *hop* heterozygous *Pak* mutant ovarioles show this phenotype). Note the side-by-side oocytes in G,I. (J) Same egg chamber as in (I) stained with anti-HtsRC antibody. The enlarged view of the two oocytes rotated 90° shows that each oocyte has four ring canals (arrowheads). (K) Schematic showing how *Pak* mutant side-by-side cyst encapsulation could be carried out by four FSCs. In an *hh* or *hop* mutant background, a reduction in FSC number and/or activity leads to incomplete separate encapsulation. (L-L″) Phenotype of cysts on side of an aberrant stalk due to *Pak* mutant clones (marked by absence of GFP). Note that oldest cyst has been encapsulated by largely wild-type follicle cells, suggesting presence of two wild-type FSCs, whereas younger cysts have been encapsulated by a mixture of wild-type and mutant follicle cells, suggesting presence of an additional, mutant FSC. Scale bars: 30 µm in A for A-E; 50 µm in F for F-J,L-L″.

required to generate the phenotype (Fig. 4A). The escort cells, a somatic cell population in the germarium, were consistently *Pak* mutant in the affected ovarioles (Fig. 4A). To confirm that loss of Pak in somatic cells was causing the paired egg chamber phenotype, we used the somatic cell-specific Gal4 lines *c587-Gal4* (Kai and Spradling, 2003), *Bab1-Gal4* (Bolívar et al., 2006) and *TJ-Gal4* (Hayashi et al., 2002; Li et al., 2003; Tanentzapf et al., 2007) to drive *Pak* RNAi transgene expression. With all drivers, *Pak* RNAi expression produced paired egg chambers (Fig. 4B-E). All of these drivers are expressed throughout ovary development, beginning in the larval ovary, thus suggesting that loss of Pak in somatic cells during ovarian development leads to the side-by-side encapsulation of egg chambers. Further analysis of ovaries in which *Pak* RNAi had been expressed with *TJ-Gal4* showed additional parallels to our results from *Pak* mutant ovaries. A similar distribution of phenotypes was seen, including the ‘unpaired egg chamber on side of stalk’ phenotype, the frequency of which, as in *Pak* mutants, was higher in older flies (supplementary material Table S2; Fig. 4E). *Pak* RNAi expression also generated paired cysts that were either only partially separately encapsulated or packaged together in a single follicular epithelium (Fig. 4F,G). These phenotypes are similar to those seen in *Pak* mutants heterozygous for *hh* or *hop* alleles.

We used the temperature-sensitive Gal4 repressor Gal80ts to analyze when loss of Pak generates the paired egg chamber phenotype (McGuire et al., 2004). Gal80ts repression of *TJ-Gal4* expression of *Pak* RNAi during pre-adult stages was achieved by maintaining the cross at a permissive temperature of 18°C until eclosion. After eclosion, adults were shifted to the restrictive temperature of 29°C for two days, thus enabling *Pak* RNAi expression, and ovaries were dissected. Only 2% of ovarioles (n=98) from these individuals showed egg chamber pairing throughout the ovariole, compared with 22-47% of ovarioles from flies in which *TJ-Gal4* expression of *Pak* RNAi had never been repressed. We conclude that loss of Pak in pre-adult somatic cells causes a paired ovariole phenotype.

Development (2015) 142, 82-91 doi:10.1242/dev.111039

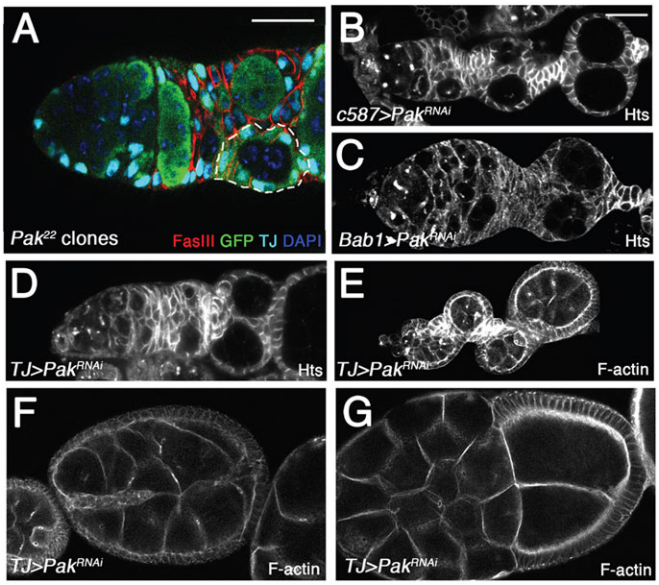

Fig. 4. The side-by-side egg chamber phenotype is caused by loss of Pak in somatic cells. Anterior is to the left in all panels. (A) Pak^{22} clones induced in third-instar larvae. Sample was stained with DAPI (blue) to mark all nuclei, with anti-TJ (light blue) to mark somatic nuclei, with anti-FasIII (red) to mark follicle cells and with anti-GFP (green) to mark wild-type cells. Note lack of GFP staining in somatic cells in region1/2a, indicating widespread loss of Pak in somatic cells of germarium. One of the cysts is encapsulated by wild-type follicle cells (highlighted by dashed line), indicating that not all FSCs need to be *Pak* mutant to generate the side-by-side egg chamber phenotype. (B-D) Expression of a Pak^{RNAi} transgene with the somatic cell drivers *c587-Gal4* (B), *Bab1-Gal4* (C) or *TJ-Gal4* (D) results in side-by-side egg chambers. Samples were stained with anti-Hts 1B1 antibody. (E-G) Phalloidin-stained ovarioles from adults in which Pak^{RNAi} transgene was expressed with *TJ-Gal4*. (E) Cysts on side of aberrant stalk phenotype, similar to that seen in *Pak* mutants. (F,G) Side-by-side cysts separated by a partial bilayered epithelium (F) or packaged into a single follicular epithelium (G), phenotypes similar to those seen when *Pak* mutants are made heterozygous for *hop* or *hh* alleles. Scale bars: 50 µm.

Cell intercalation does not occur properly during basal stalk formation in *Pak* mutant ovaries

In an effort to identify the origin of the side-by-side egg chamber phenotype, we examined *Pak* mutant larval and pupal ovaries for defects, and, whereas larval to mid-pupal ovaries showed no obvious abnormalities (supplementary material Fig. S1), late-pupal ovaries were clearly abnormal, in that the basal stalks had not formed properly (Figs 5 and 6). The segregation of cells in the pupal ovary into individual ovarioles is initiated by the posterior migration of the apical cells between the terminal filaments and onwards, dividing the somatic basal stalk precursor cells into clusters of cells (Godt and Laski, 1995; King, 1970). These cells flatten and intercalate into a transient structure called the basal stalk that is initially two cell diameters wide, with the outer edges of the cells in contact with the basement membrane. This structure later resolves into what is largely a single column of cells in contact with the first germline cyst produced in that ovariole (Fig. 5A). Pak was expressed in both the germline cyst and the basal stalk in the pupal ovary (Fig. 5A, inset). The basal stalk failed to resolve into a single column of cells in *Pak* mutant ovaries, and stalks were short and wide, frequently contacting two germline cysts at a time instead of the usual one (Fig. 6A-A″). We measured the width of basal stalks at the point of contact with germline cysts and found that *Pak* mutant stalks were twice as wide as WT (supplementary material Fig. S2). The formation of the basal stalk is an example of a mesenchymal cell intercalation with parallels to notochord cell intercalation in *Xenopus* (Keller, 2006). Basal stalk formation remains largely uncharacterized, and we examined the wild-type process in more detail in the hope of gaining insight into the mechanism of cell intercalation and the putative role of Pak. By staining for the basal marker βPS-integrin we confirmed that the basal stalk is surrounded by basement membrane (Fig. 5B). The structure of the mature basal stalk suggests a transition from mesenchymal cells to an epithelium and we looked for the formation of adherens junctions by staining for DE-Cadherin. Close examination of the basal stalk revealed three distinct cell organizations that are probably different stages in the intercalation process. The cells at the anterior end of the basal stalk remained as two columns, but were linked by adherens junctions at their inward-facing edges (Fig. 5C-E″). In the middle of the stalk, cells were organized into a single column of bottle-shaped cells, with their constriction beginning at about the position of the adherens junction (Fig. 5F). Finally, the posterior end of the basal stalk consisted of disk-shaped cells in a single column (Fig. 5A, arrowhead). The basal stalk cells that were organized into a single column constituted an epithelium with a unique organization, which was best visualized in cross-sectional views of the basal stalk (Fig. 5G-K). Cells were linked by a spot adherens junction in their middle that was surrounded by the basolateral marker FasIII, and the cell cortex was ringed by basement membrane.

Pak mutant basal stalks were two cells wide for their entire length, remaining as two columns of cells linked by adherens junctions at their inward-facing edges, suggesting a failure of cell intercalation (Fig. 6A-C″). A requirement for Pak in basal stalk cell intercalation is consistent with its established roles in regulating the actin cytoskeleton during cell shape change and motility (Bokoch, 2003). We have shown that Pak regulates actomyosin contractility during development of the follicular epithelium, and it is possible that misregulation of contractility underlies the *Pak* basal stalk phenotype (Vlachos and Harden, 2011). We assessed the status of actomyosin contractility in basal stalks by staining for phosphorylated myosin light chain (pMLC), which reveals active myosin. Interestingly, the pMLC distribution in wild-type basal stalks indicated dynamic regulation of actomyosin contractility, with some cells devoid of pMLC and others with very high levels (Fig. 5M-M″ and Fig. 6D). By contrast, a weak, uniform distribution of pMLC was seen in *Pak* mutant basal stalks (Fig. 6E).

The results of our analysis of basal stalk formation suggest that the paired ovariole phenotype in *Pak* mutants originates in the late pupal stage. The small number of paired ovarioles seen when *Pak* RNAi was expressed only in the adult might be due to leaky Gal80ts repression (Kamikouchi et al., 2009) and/or 'lagging' ovarioles, in which basal stalk development persisted into adulthood. With regard to the latter, we and others have observed basal stalks in the ovarioles of newly eclosed females (Smith et al., 2002; and data not shown), and it is possible that basal stalk cell intercalation still occurs in some adult ovaries.

Pak mutant ovaries have short, wide germaria with a reduced number of escort cells

We extended our analysis of the effects of Pak on somatic cell specification by examining somatic cells in the germarium, using the enhancer trap *PZ1444*, which positively marks the cap cells and escort cells (Decotto and Spradling, 2005; Kai and Spradling, 2003). We found that wild-type germaria had an average of 29 escort cells, whereas *Pak* mutant germaria had an average of 15 escort cells (Fig. 6F,G; supplementary material Table S3). Wild-

Development (2015) 142, 82-91 doi:10.1242/dev.111039

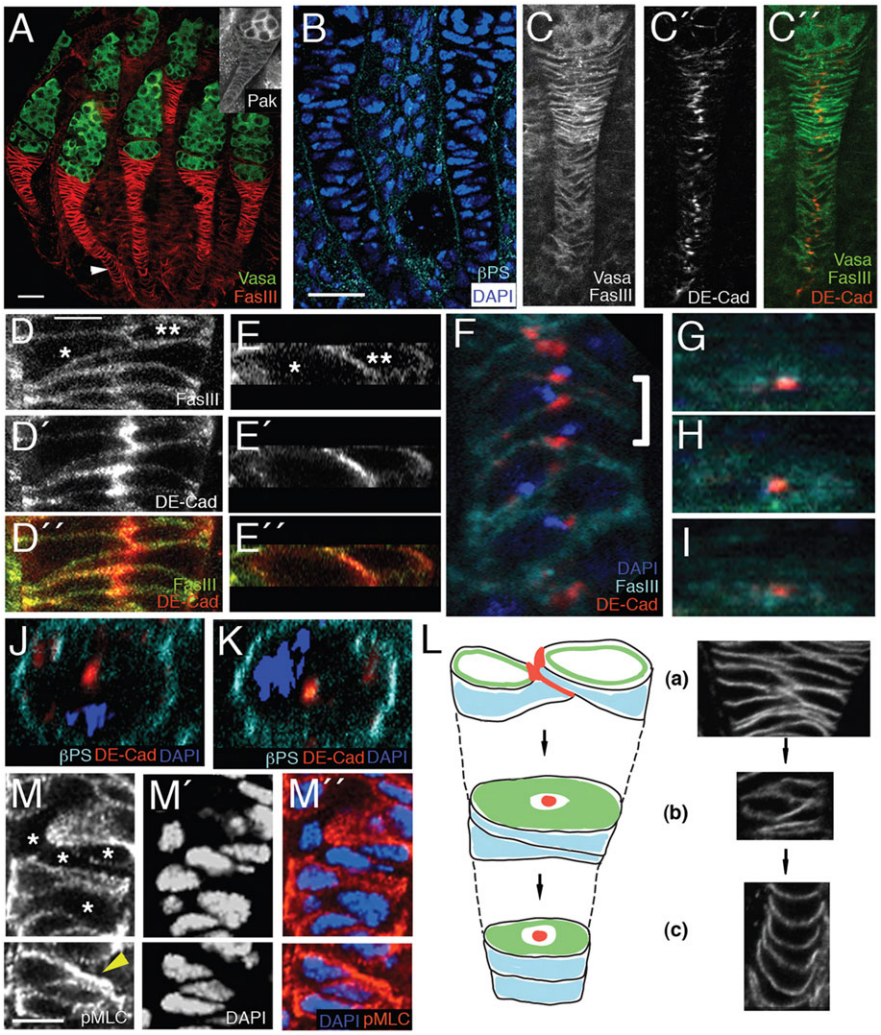

Fig. 5. Cell intercalation in the pupal ovary forms a basal stalk with a novel radial cell polarity. (A-M″) Pupal ovaries 40 h after puparium formation (APF). Anterior end of each ovary is at the top. (A) Wild-type pupal ovary stained with anti-Vasa (green) to mark germ cells and with anti-FasIII (red) to mark basal stalk cells. Basal stalks are two cells wide at the anterior end of stalk where they contact the germ cells, but a single cell wide for most of their length, with bottle-shaped cells in the middle and disk-shaped cells at the posterior end (arrowhead). Inset shows anti-Pak staining of pupal ovary. Pak is expressed in basal stalk and germline cells. (B) Wild-type basal stalks stained with anti-βPS integrin to show that basal stalks are surrounded by basement membrane. (C-C″) Wild-type basal stalks stained with anti-DE-Cadherin (red) to mark adherens junctions and with anti-Vasa and anti-FasIII to reveal cells (green). There are adherens junctions where cells contact each other in the two-cell-wide proportion of the basal stalk and adherens junctions between cells in the single-cell-wide proportion. (D-D″) High-magnification view of adherens junction between two cells (asterisks) in two-cell-wide proportion of wild-type basal stalk. (E-E″) Cross-sectional view of same cells as in D-D″. (F) Bottle-shaped cells in wild-type basal stalk stained with DAPI (blue) to mark nuclei and anti-FasIII (cyan) and anti-DE-Cadherin (red), showing 'yin-yang' arrangement, in which narrow end of one cell is in contact with wide end of its neighbors. (G-I) Bottle-shaped cells marked by the bracket in F, viewed in cross-section. Cells contain a dot of DE-cadherin staining surrounded by FasIII staining. (J,K) Neighboring disk-shape cells from a basal stalk showing DE-Cadherin at center of disk (red) and basal marker βPS integrin (cyan) circumferentially distributed. Nuclei are stained with DAPI (blue). The distribution of polarity markers in G-K indicates a radial cell polarity. (L) Schematic showing the three types of cell organization in the basal stalk. Red, DE-Cadherin; green, FasIII; blue, βPS integrin. (a) At the anterior end the stalk is two cells wide, with adherens junction at point of contact. (b) In the middle of stalk, cells are bottle-shaped in side view and linked by spot adherens junctions. (c) At the posterior end of stalk cells are disk-shaped. Note the radial cell polarity in (b) and (c). We propose that the three types of organization are stages in the intercalation process (arrows). (M-M″) Wild-type basal stalk stained with anti-pMLC and DAPI. Some cells show no pMLC staining (asterisks), whereas others show high levels. Cell marked with arrowhead in K shows high level of pMLC in constricted region. Scale bars: 10 μm in A,B for A-C″; 2 μm in D for D-K; 4 μm in M for M-M″.

type and *Pak* mutant germaria had similar numbers of germline cysts (supplementary material Table S3), indicating that the ratio of escort cell number to number of germline cysts had been halved in *Pak* mutant germaria. Accompanying the reduction in escort cell number in *Pak* mutant germaria were a significant shortening of region 1/2a of the germarium along the anterior-posterior axis and a significant widening of the germarium (supplementary material Table S3). These results suggest that basal stalk widening, reduction in escort cell number and resulting increase in FSC number lead to a wide germarium with a short anterior region in which cysts can be encapsulated two at a time using anteriorly displaced FSC niches.

DISCUSSION

Pak is required for cell intercalation during basal stalk formation leading to a column of cells with unique radial cell polarity

Based on our observations, we propose a model for cell intercalation in the basal stalk (Fig. 5L). Mesenchymal cells organize themselves

Development (2015) 142, 82-91 doi:10.1242/dev.111039

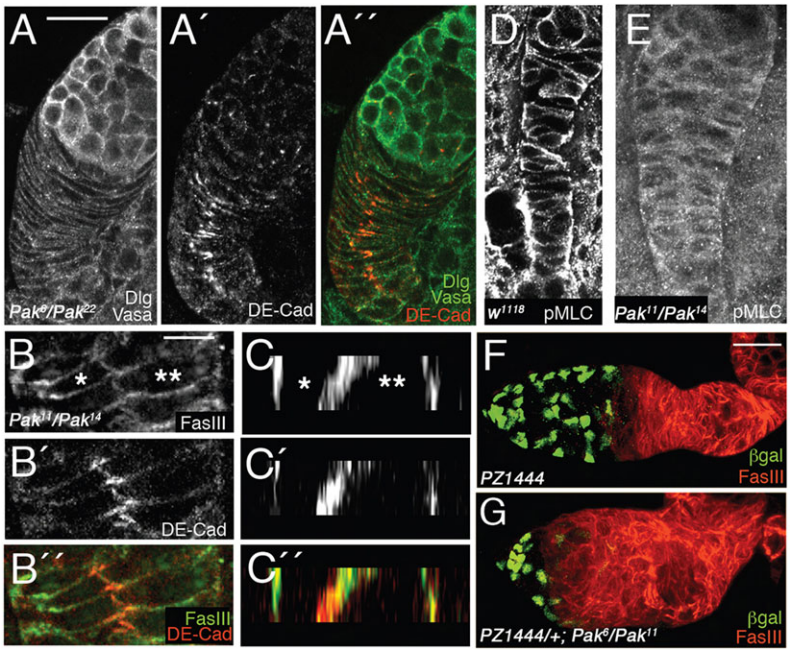

Fig. 6. Cell intercalation fails in *Pak* mutant pupal ovaries, resulting in wide basal stalks. (A,B) Pupal ovaries 40 h APF. Anterior end of each ovary is at the top. (D,E) Adult germaria. Anterior end is to the left. (A-A″) Single Pak^{6}/Pak^{22} basal stalk stained with anti-Vasa and anti-Dlg (both in green) and anti-DE-cadherin (red). Cells are very flat and wide and have failed to intercalate, forming an abnormally wide basal stalk. (B-B″) High-magnification view of adherens junction between two cells (asterisks) at posterior end of Pak^{11}/Pak^{14} basal stalk. (C-C″) Cross-sectional view of same cells as in B-B″. (D) pMLC distribution in wild-type basal stalk. (E) Pak^{11}/Pak^{14} basal stalk showing abnormal pMLC staining. (F,G) Adult wild-type (F) and Pak^{6}/Pak^{11} (G) germaria carrying the enhancer trap *PZ1444*, stained with β-galactosidase (green) to mark cap cells and escort cells and with anti-FasIII (red) to mark follicle cells and thus reveal region 2b. Compared with wild-type, the Pak^{6}/Pak^{11} germarium is wider, with a shorter region 1/2a and fewer escort cells. Scale bars: 10 µm in A,B; 30 µm in F. See also supplementary material Fig. S2 and Table S3.

into two columns, migrate toward each other, begin intercalating and form adherens junctions. A commonly used mechanism for epithelial morphogenesis is apical constriction of cells by an actomyosin contractile apparatus anchored to adherens junctions (Sawyer et al., 2010). In a typical epithelium, in which cells are all oriented in the same direction, apical constriction causes bending of the tissue. However, in the basal stalk, constriction of cells organized in alternating directions could drive the transition from partial intercalation into a single column of bottle-shaped cells. Release of this constriction would then lead to the final morphology of disk-shaped cells, with the basal stalk lengthening similar to a bellows being opened up. Stalk cells showing high levels of pMLC in our immunohistochemistry might have been caught in the midst of constricting, whereas those with low levels were not actively changing shape. The cell intercalation during basal stalk formation might serve as a mechanism for pulling the protein meshwork of the basement membrane inwards, acting as a 'corset' to compress the entire developing ovariole into a long, narrow structure, in which germline cysts are encapsulated one at a time. In support of this model are results suggesting that, in primitive streak formation in the quail, intercalating cells drag the extracellular matrix toward the midline (Zamir et al., 2008). In *Pak* mutant ovarioles, actomyosin constriction is misregulated and the resulting failure to complete intercalation leads to a short, wide germarium, which, as discussed below, can encapsulate two cysts at a time.

When viewed in cross-section, the one-cell-wide column of basal stalk cells reveals a unique organization of round, flat cells, linked together by a spot adherens junction in their middle. We describe this organization as 'radial cell polarity', in that proteins that are normally distributed along the apicobasal axis of an epithelial cell are radially localized in the same plane, with the normally apical adherens junction in the middle, and basolateral and basal proteins circumferentially distributed. To our knowledge, this cellular organization has not been previously described, although the term 'radial cell polarity' has been used to describe the localization of Rho-associated kinase and myosin to the middle of the apical cortex of ventral furrow cells during *Drosophila* gastrulation (Mason et al., 2013). The radial cell polarity in the basal stalk presumably results from the cell intercalation process. Adherens junctions are initially established between the inward-facing edges of cells. The cells then 'spread out' from these junctions to form a column of cells one cell wide, which leaves the adherens junction in the middle of each cell (Fig. 5L).

In which cells does loss of Pak cause the wide basal-stalk phenotype and, consequently, side-by-side encapsulation of cysts? We suspect that Pak functions in the basal stalk cells to regulate cell intercalation in a cell-autonomous fashion and that it is loss of this activity that causes the phenotypes. If this is the case, generating the paired egg-chamber phenotype with *Pak* clones would require loss of Pak in precursor cells upstream of basal stalk cell proliferation. Consistent with this, paired ovarioles resulting from *Pak* clones are derived from germaria with largely *Pak* mutant somatic cells (Fig. 4A), which could be due to loss of Pak in early somatic cell precursors, the descendants of which include the basal stalk and escort cells.

A model for positioning of the FSC niche

Taking our data into consideration with previous studies, we have developed a model for positioning of the FSC niche (Fig. 7). The FSC niche must be ready to encapsulate the first germline cyst that matures in the pupal ovary. One way to ensure this is to have cyst maturation initiating development of the niche. The escort cells form a component of the niche and their long cellular processes can only develop in the presence of differentiated germ cells (Kirilly et al., 2011; Nystul and Spradling, 2007; Sahai-Hernandez and Nystul, 2013; Song and Xie, 2002). We propose that contact of a mature germline cyst with the basal stalk is required for formation of a pair of FSC niches. The posterior-most extent of cyst positioning, and hence location of the FSC niches, is determined by the basal stalk, which immobilizes the first germline cyst. Maturation of the first cyst enables process extension by neighboring escort cells, which then contributes to niche formation. Two cells, possibly escort cells or a common escort/FSC precursor, on opposite sides of the cyst from each other, are destined to become FSCs. These cells are established and maintained as FSCs through the formation of DE-Cadherin-based adhesion to neighboring escort cells (Song and Xie, 2002) and integrin-based adhesion to LanA, secreted by themselves and their daughters (O'Reilly et al., 2008).

Development (2015) 142, 82-91 doi:10.1242/dev.111039

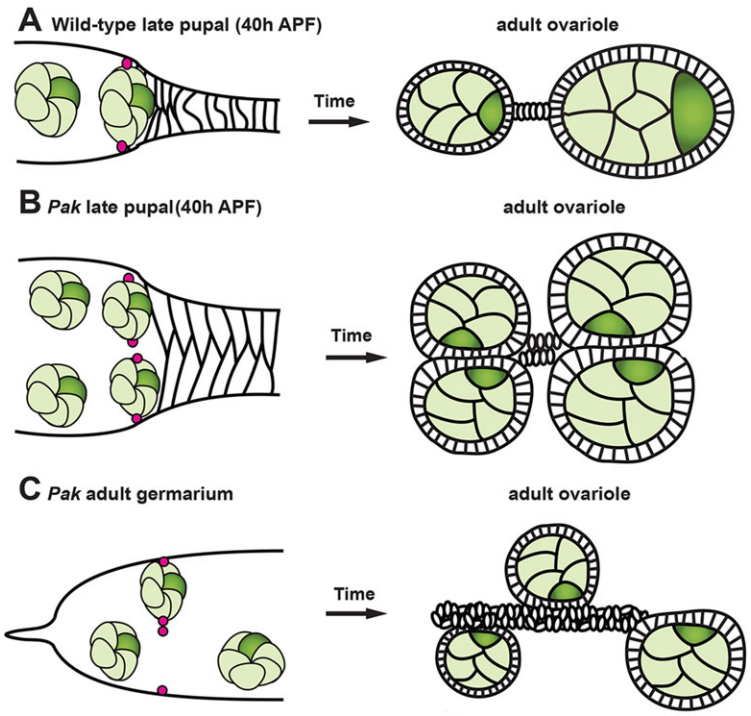

Fig. 7. A model for formation of the FSC niche and derivation of *Pak* mutant phenotypes. Anterior is to the left in all panels. (A) Development of wild-type ovariole. Mature germline cyst at tip of the basal stalk in the pupal ovary guides establishment of two FSC niches containing FSCs (magenta). Cysts are encapsulated one at a time in the resulting germarium. (B) Development of *Pak* mutant ovariole. Due to a failure in cell intercalation, *Pak* mutants form abnormally wide basal stalks, enabling side-by-side cysts and the anchoring of four FSCs in at least three niches (the two internal FSCs might share a niche). The resulting germarium is capable of encapsulating two cysts at a time. (C) As the *Pak* mutant germarium ages, the side-by-side cysts become unsynchronized and are packaged individually, resulting in the phenotype of unpaired cysts on either side of an aberrant stalk.

In the case of *Pak* mutant ovarioles, the wide basal stalk forms a second 'cyst-docking station', allowing a second cyst to direct specification of a second pair of FSCs, possibly at the expense of escort cells (Fig. 7B). Visual evidence for the existence of these FSCs comes from the detection of extra Cas-positive, FasIII-negative cells as well as ectopic LanA in *Pak* mutant germaria. The extra FSCs in the *Pak* mutant germarium are remarkably efficient at carrying out the individual encapsulation of paired cysts, with packaging of paired cysts into a single follicular epithelium only occurring when FSC activity is impaired by heterozygosity for *hh* or *hop*. Similarly, when Pak function is impaired by RNAi expression with *TJ-Gal4*, most paired cysts are encapsulated individually, although occasional packaging of two cysts in one follicular epithelium does occur (Fig. 4G). The *Pak* mutant germarium appears unable to sustain the flow of side-by-side cysts through the two pairs of FSCs, and some cysts get encapsulated without a partner. Strikingly, as the flies age, the phenotype of unpaired cysts on either side of an aberrant stalk becomes more prevalent. We suggest that this phenotype is due to a period of only one pair of FSCs at a time being used for cyst encapsulation, with extra follicle cells produced by the 'unused' FSCs contributing to formation of the aberrant stalk (Fig. 7C). The unpaired cysts are found on one side or the other of the aberrant stalk, depending on which pair of FSCs was used.

We propose that, in the *Pak* mutant pupal ovary, cells that would normally contribute to the escort cell population are redirected to become FSCs in supernumerary niches, and that this might explain the reduced number of escort cells compared with WT. Escort cells play an active role in transporting cysts through the germarium (Decotto and Spradling, 2005; Morris and Spradling, 2011). The successful encapsulation of germline cysts despite a paucity of escort cells in *Pak* mutants might be due to the fact that the escort cells are frequently transporting two cysts at a time instead of the usual one. In addition, the escort cells need not transport the cysts as far as in wild-type germaria, as regions 1 and 2a are shortened.

A recent study proposed that the FSC niche is regulated by intersecting gradients of ligands for signaling pathways, including Hh and JAK-STAT (Vied et al., 2012), and these probably work together with germline cyst contact to specify which cells can become FSCs. Elevated JAK-STAT signaling leads to what appear to be supernumerary FSCs in ectopic positions, similar to what we see in *Pak* mutants (Vied et al., 2012). In the case of elevated JAK-STAT, the recruitment of more cells as FSCs might be due to more cells experiencing the appropriate internal level of pathway activation, whereas in *Pak* mutant germaria, more cells are positioned to respond to ligands and become FSCs.

The FSC is faced with a unique challenge in that it must generate an epithelium to package a 'moving target', the germline cyst. Having the germline cyst position the FSC niche ensures that the niche always forms in a position in line with the flow of cysts from the anterior of the germarium. Our results indicate that the FSC can function normally to produce follicle cells even when in a mispositioned niche. Our analysis of *Pak* mutant ovarioles demonstrates that the position and number of FSC niches can vary in the germarium and yet all the cysts that pass through still get encapsulated into their own follicular epithelium. Our data suggest that *Pak* mutant germaria with paired follicles have at least three FSC niches (two lateral niches and one internal niche), and possibly four separate niches, one for each FSC. The remarkable plasticity of the FSC niche enables encapsulation of two cysts at a time in the *Pak* mutant ovary.

There is evidence in mammals for the association of precursors of epithelial stem cells with germ cells prior to follicle formation. During mammalian oogenesis the oocyte becomes encased in a single layer of several precursor epithelial granulosa cells to form the primordial follicle (Pepling, 2006). This layer of cells has been proposed to contain resting granulosa stem cells that, following activation of the follicle, produce a follicular epithelium that encases the oocyte during the formation of the mature follicle (Lavranos et al., 1999; Rodgers et al., 1999). Our proposed association of precursor FSCs with the germline cyst in the pupal ovary could be considered the *Drosophila* equivalent of the primordial follicle, and

Development (2015) 142, 82-91 doi:10.1242/dev.111039

it would be of interest to determine if there are parallels between flies and mammals in the specification of the stem cell niche that drives formation of the follicular epithelium.

MATERIALS AND METHODS

Drosophila stocks and somatic clone analysis

Pak^{RNAi} flies were from the Vienna Drosophila RNAi Center (Vienna, Austria), Pak^{6}, Pak^{11} and Pak^{22} flies from H. Hing (State University of New York at Brockport, NY, USA), *TJ-Gal4* flies from D. Godt and G. Tanentzapf (University of British Columbia, Vancouver, Canada), $rho1^{k02107rev5}$ flies from S. Parkhurst (Fred Hutchinson Cancer Research Center, Seattle, WA, USA), moe^{PL54} flies from F. Payre (CNRS, University of Toulouse, France) and the *PZ1444* enhancer trap line from A. Spradling (Carnegie Institute, Baltimore, MD, USA). All other stocks were obtained from the Bloomington Stock Center (Bloomington, USA). A w^{1118} stock was used as a wild-type control in this study. *Pak* somatic clones were induced using the FLP/FRT method (Xu and Rubin, 1993). To induce *Pak* loss-of-function clones using hsFLP, third-instar larvae from the appropriate crosses were heat-shocked at 37°C for 2 h for 3 consecutive days. Female progeny of the genotype *hsFLP;* Pak^{22}*FRT82B/UbiGFP FRT82B* were grown on media containing yeast for 2-3 days to allow for optimal development and maturation of ovaries.

Immunohistochemistry

Larval and pupal ovaries were dissected in PBS, fixed in 4% formaldehyde for 20 min, then rinsed in PBS, blocked with 0.1% PBT+0.5% BSA and stained with primary and secondary antibodies. Adult ovaries were dissected, fixed and stained as previously described (Verheyen and Cooley, 1994). Primary antibodies used in this study were monoclonal anti-BicD [1B11, Developmental Studies Hybridoma Bank (DSHB); 1:10], mouse monoclonal anti-Hts 1B1 (DSHB; 1:5), mouse monoclonal anti-HtsRC (DSHB; 1:20), mouse monoclonal anti-Fasciclin III (FasIII) (7G10, DSHB; 1:100), rabbit anti-GFP (G1544, Sigma; 1:500), rat monoclonal anti-Vasa (DSHB; 1:100), guinea pig anti-TJ (Li et al., 2003; 1:5000), rabbit anti-β-galactosidase (ab616, Abcam; 1:2000), rabbit anti-Pak (Harden et al., 1996; 1:1000), rat monoclonal anti-DE-Cadherin (DCAD2, DSHB; 1:50), mouse monoclonal anti-Dlg (DLG1, DSHB; 1:5), mouse monoclonal anti-β-PS integrin (CF.6G11, DSHB; 1:2) and rabbit anti-Castor (Chang et al., 2013; 1:500). Secondary antibodies were used at a 1:200 dilution and were conjugated to Cy5, FITC or TRITC. To visualize F-actin, ovarioles were incubated with 1:1000 FITC-conjugated phalloidin (Sigma) for 30 min with rotation. Samples were mounted in VECTASHIELD Mounting Medium with DAPI (Vector Laboratories). Images were acquired using Zeiss LSM 410 or Nikon A1R laser-scanning confocal microscopes or a Zeiss ApoTome structured-illumination microscope and processed using Adobe Photoshop.

Acknowledgements

We thank Hong Yu for the original observation of the *Pak* side-by-side egg chamber phenotype, D. Godt, H. Hing, S. Parkhurst, F. Payre, A. Spradling and G. Tanentzapf for fly stocks, D. Godt, W. Odenwald and the Developmental Studies Hybridoma Bank for antibodies, D. Godt for advice on pupal ovary dissections, and N. Hawkins and E. Verheyen for discussions and comments on the manuscript.

Competing interests

The authors declare no competing financial interests.

Author contributions

S.V., R.C., T.N. and N.H. designed the experiments; S.V., R.C., S.J. and M.C. performed the experiments; and S.V. and N.H. wrote the manuscript.

Funding

This work was supported by a Natural Sciences and Engineering Research Council of Canada grant [RGPIN217532 to N.H.].

Supplementary material

Supplementary material available online at
http://dev.biologists.org/lookup/suppl/doi:10.1242/dev.111039/-/DC1

References

Assa-Kunik, E., Torres, I. L., Schejter, E. D., Johnston, D. S. and Shilo, B.-Z. (2007). Drosophila follicle cells are patterned by multiple levels of Notch signaling and antagonism between the Notch and JAK/STAT pathways. *Development* **134**, 1161-1169.

Berns, N., Woichansky, I., Friedrichsen, S., Kraft, N. and Riechmann, V. (2014). A genome-scale in vivo RNAi analysis of epithelial development in Drosophila identifies new proliferation domains outside of the stem cell niche. *J. Cell Sci.* **127**, 2736-2748.

Bokoch, G. M. (2003). Biology of the p21-activated kinases. *Annu. Rev. Biochem.* **72**, 743-781.

Bolívar, J., Pearson, J., López-Onieva, L. and González-Reyes, A. (2006). Genetic dissection of a stem cell niche: the case of the Drosophila ovary. *Dev. Dyn.* **235**, 2969-2979.

Chang, Y.-C., Jang, A. C.-C., Lin, C.-H. and Montell, D. J. (2013). Castor is required for Hedgehog-dependent cell-fate specification and follicle stem cell maintenance in Drosophila oogenesis. *Proc. Natl. Acad. Sci. USA* **110**, E1734-E1742.

Chen, H.-J., Wang, C.-M., Wang, T.-W., Liaw, G.-J., Hsu, T.-H., Lin, T.-H. and Yu, J.-Y. (2011). The Hippo pathway controls polar cell fate through Notch signaling during Drosophila oogenesis. *Dev. Biol.* **357**, 370-379.

Conder, R., Yu, H., Zahedi, B. and Harden, N. (2007). The serine/threonine kinase dPak is required for polarized assembly of F-actin bundles and apical-basal polarity in the Drosophila follicular epithelium. *Dev. Biol.* **305**, 470-482.

Decotto, E. and Spradling, A. C. (2005). The Drosophila ovarian and testis stem cell niches: similar somatic stem cells and signals. *Dev. Cell* **9**, 501-510.

Forbes, A. J., Lin, H., Ingham, P. W. and Spradling, A. C. (1996a). hedgehog is required for the proliferation and specification of ovarian somatic cells prior to egg chamber formation in Drosophila. *Development* **122**, 1125-1135.

Forbes, A. J., Spradling, A. C., Ingham, P. W. and Lin, H. (1996b). The role of segment polarity genes during early oogenesis in Drosophila. *Development* **122**, 3283-3294.

Frydman, H. M. and Spradling, A. C. (2001). The receptor-like tyrosine phosphatase Lar is required for epithelial planar polarity and for axis determination within Drosophila ovarian follicles. *Development* **128**, 3209-3220.

Godt, D. and Laski, F. A. (1995). Mechanisms of cell rearrangement and cell recruitment in Drosophila ovary morphogenesis and the requirement of bric a brac. *Development* **121**, 173-187.

Gonzalez-Reyes, A. and St Johnston, D. (1998). The Drosophila AP axis is polarised by the cadherin-mediated positioning of the oocyte. *Development* **125**, 3635-3644.

Harden, N., Lee, J., Loh, H. Y., Ong, Y. M., Tan, I., Leung, T., Manser, E. and Lim, L. (1996). A Drosophila homolog of the Rac- and Cdc42-activated serine/threonine kinase PAK is a potential focal adhesion and focal complex protein that colocalizes with dynamic actin structures. *Mol. Cell. Biol.* **16**, 1896-1908.

Hartman, T. R., Zinshteyn, D., Schofield, H. K., Nicolas, E., Okada, A. and O'Reilly, A. M. (2010). Drosophila Boi limits Hedgehog levels to suppress follicle stem cell proliferation. *J. Cell Biol.* **191**, 943-952.

Hartman, T. R., Strochlic, T. I., Ji, Y., Zinshteyn, D. and O'Reilly, A. M. (2013). Diet controls Drosophila follicle stem cell proliferation via Hedgehog sequestration and release. *J. Cell Biol.* **201**, 741-757.

Hayashi, S., Ito, K., Sado, Y., Taniguchi, M., Akimoto, A., Takeuchi, H., Aigaki, T., Matsuzaki, F., Nakagoshi, H., Tanimura, T. et al. (2002). GETDB, a database compiling expression patterns and molecular locations of a collection of Gal4 enhancer traps. *Genesis* **34**, 58-61.

Hongay, C. F. and Orr-Weaver, T. L. (2011). Drosophila Inducer of MEiosis 4 (IME4) is required for Notch signaling during oogenesis. *Proc. Natl. Acad. Sci. USA* **108**, 14855-14860.

Horne-Badovinac, S. and Bilder, D. (2005). Mass transit: epithelial morphogenesis in the Drosophila egg chamber. *Dev. Dyn.* **232**, 559-574.

Kai, T. and Spradling, A. (2003). An empty Drosophila stem cell niche reactivates the proliferation of ectopic cells. *Proc. Natl. Acad. Sci. USA* **100**, 4633-4638.

Kamikouchi, A., Inagaki, H. K., Effertz, T., Hendrich, O., Fiala, A., Göpfert, M. C. and Ito, K. (2009). The neural basis of Drosophila gravity-sensing and hearing. *Nature* **458**, 165-171.

Keller, R. (2006). Mechanisms of elongation in embryogenesis. *Development* **133**, 2291-2302.

King, R. C. (1970). *Ovarian Development in Drosophila melanogaster*. New York: Academic Press.

Kirilly, D., Wang, S. and Xie, T. (2011). Self-maintained escort cells form a germline stem cell differentiation niche. *Development* **138**, 5087-5097.

Lavranos, T. C., Mathis, J. M., Latham, S. E., Kalionis, B., Shay, J. W. and Rodgers, R. J. (1999). Evidence for ovarian granulosa stem cells: telomerase activity and localization of the telomerase ribonucleic acid component in bovine ovarian follicles. *Biol. Reprod.* **61**, 358-366.

Li, M. A., Alls, J. D., Avancini, R. M., Koo, K. and Godt, D. (2003). The large Maf factor Traffic Jam controls gonad morphogenesis in Drosophila. *Nat. Cell Biol.* **5**, 994-1000.

Li, Q., Xin, T., Chen, W., Zhu, M. and Li, M. (2008). Lethal(2)giant larvae is required in the follicle cells for formation of the initial AP asymmetry and the oocyte polarity during Drosophila oogenesis. *Cell Res.* **18**, 372-384.

López-Schier, H. and St Johnston, D. (2001). Delta signaling from the germ line controls the proliferation and differentiation of the somatic follicle cells during Drosophila oogenesis. *Genes Dev.* **15**, 1393-1405.
Losick, V. P., Morris, L. X., Fox, D. T. and Spradling, A. (2011). Drosophila stem cell niches: a decade of diskovery suggests a unified view of stem cell regulation. *Dev. Cell* **21**, 159-171.
Mason, F. M., Tworoger, M. and Martin, A. C. (2013). Apical domain polarization localizes actin-myosin activity to drive ratchet-like apical constriction. *Nat. Cell Biol.* **15**, 926-936.
Mata, J., Curado, S., Ephrussi, A. and Rørth, P. (2000). Tribbles coordinates mitosis and morphogenesis in Drosophila by regulating string/CDC25 proteolysis. *Cell* **101**, 511-522.
McCaffrey, R., St Johnston, D. and González-Reyes, A. (2006). A novel mutant phenotype implicates dicephalic in cyst formation in the Drosophila ovary. *Dev. Dyn.* **235**, 908-917.
McGuire, S. E., Mao, Z. and Davis, R. L. (2004). Spatiotemporal gene expression targeting with the TARGET and gene-switch systems in Drosophila. *Sci. STKE* **2004**, pl6.
Morris, L. X. and Spradling, A. C. (2011). Long-term live imaging provides new insight into stem cell regulation and germline-soma coordination in the Drosophila ovary. *Development* **138**, 2207-2215.
Muzzopappa, M. and Wappner, P. (2005). Multiple roles of the F-box protein Slimb in Drosophila egg chamber development. *Development* **132**, 2561-2571.
Nystul, T. and Spradling, A. (2007). An epithelial niche in the Drosophila ovary undergoes long-range stem cell replacement. *Cell Stem Cell* **1**, 277-285.
Nystul, T. and Spradling, A. (2010). Regulation of epithelial stem cell replacement and follicle formation in the Drosophila ovary. *Genetics* **184**, 503-515.
O'Reilly, A. M., Ballew, A. C., Miyazawa, B., Stocker, H., Hafen, E. and Simon, M. A. (2006). Csk differentially regulates Src64 during distinct morphological events in Drosophila germ cells. *Development* **133**, 2627-2638.
O'Reilly, A. M., Lee, H.-H. and Simon, M. A. (2008). Integrins control the positioning and proliferation of follicle stem cells in the Drosophila ovary. *J. Cell Biol.* **182**, 801-815.
Pepling, M. E. (2006). From primordial germ cell to primordial follicle: mammalian female germ cell development. *Genesis* **44**, 622-632.
Rodgers, R. J., Lavranos, T. C., van Wezel, I. L. and Irving-Rodgers, H. F. (1999). Development of the ovarian follicular epithelium. *Mol. Cell. Endocrinol.* **151**, 171-179.
Sahai-Hernandez, P. and Nystul, T. G. (2013). A dynamic population of stromal cells contributes to the follicle stem cell niche in the Drosophila ovary. *Development* **140**, 4490-4498.
Sahai-Hernandez, P., Castanieto, A. and Nystul, T. G. (2012). Drosophila models of epithelial stem cells and their niches. *Wiley Interdiscip. Rev. Dev. Biol.* **1**, 447-457.
Sahut-Barnola, I., Godt, D., Laski, F. A. and Couderc, J.-L. (1995). Drosophila ovary morphogenesis: analysis of terminal filament formation and identification of a gene required for this process. *Dev. Biol.* **170**, 127-135.
Sawyer, J. M., Harrell, J. R., Shemer, G., Sullivan-Brown, J., Roh-Johnson, M. and Goldstein, B. (2010). Apical constriction: a cell shape change that can drive morphogenesis. *Dev. Biol.* **341**, 5-19.
Shyu, L.-F., Sun, J., Chung, H.-M., Huang, Y.-C. and Deng, W.-M. (2009). Notch signaling and developmental cell-cycle arrest in Drosophila polar follicle cells. *Mol. Biol. Cell* **20**, 5064-5073.
Smith, J. E., III, Cummings, C. A. and Cronmiller, C. (2002). Daughterless coordinates somatic cell proliferation, differentiation and germline cyst survival during follicle formation in Drosophila. *Development* **129**, 3255-3267.
Song, X. and Xie, T. (2002). DE-cadherin-mediated cell adhesion is essential for maintaining somatic stem cells in the Drosophila ovary. *Proc. Natl. Acad. Sci. USA* **99**, 14813-14818.
Song, X. and Xie, T. (2003). Wingless signaling regulates the maintenance of ovarian somatic stem cells in *Drosophila*. *Development* **130**, 3259-3268.
Spradling, A. C., Nystul, T., Lighthouse, D., Morris, L., Fox, D., Cox, R., Tootle, T., Frederick, R. and Skora, A. (2008). Stem cells and their niches: integrated units that maintain Drosophila tissues. *Cold Spring Harb. Symp. Quant. Biol.* **73**, 49-57.
Tanentzapf, G., Devenport, D., Godt, D. and Brown, N. H. (2007). Integrin-dependent anchoring of a stem-cell niche. *Nat. Cell Biol.* **9**, 1413-1418.
Verheyen, E. and Cooley, L. (1994). Looking at oogenesis. *Methods Cell Biol.* **44**, 545-561.
Vied, C., Reilein, A., Field, N. S. and Kalderon, D. (2012). Regulation of stem cells by intersecting gradients of long-range niche signals. *Dev. Cell* **23**, 836-848.
Vlachos, S. and Harden, N. (2011). Genetic evidence for antagonism between Pak protein kinase and Rho1 small GTPase signaling in regulation of the actin cytoskeleton during Drosophila oogenesis. *Genetics* **187**, 501-512.
Xu, T. and Rubin, G. M. (1993). Analysis of genetic mosaics in developing and adult Drosophila tissues. *Development* **117**, 1223-1237.
Zamir, E. A., Rongish, B. J. and Little, C. D. (2008). The ECM moves during primitive streak formation–computation of ECM versus cellular motion. *PLoS Biol.* **6**, e247.
Zhang, Y. and Kalderon, D. (2000). Regulation of cell proliferation and patterning in Drosophila oogenesis by Hedgehog signaling. *Development* **127**, 2165-2176.
Zhang, Y. and Kalderon, D. (2001). Hedgehog acts as a somatic stem cell factor in the Drosophila ovary. *Nature* **410**, 599-604.